ChemComm

RSC Publishing

COMMUNICATION

View Article Online
View Journal | View Issue

Temperature, light and solvent-induced spin transition in a 3D 2-fold interpenetrated PtS-type porous coordination polymer†

Cite this: *Chem. Commun.*, 2013, **49**, 10977

Received 25th July 2013,
Accepted 7th October 2013

DOI: 10.1039/c3cc45691a

www.rsc.org/chemcomm

Xiang-Yi Chen, Hai-Yan Shi, Rong-Bin Huang, Lan-Sun Zheng and Jun Tao*

A 3D 2-fold interpenetrated porous coordination polymer, $[Fe(NCS)_2(tppm)]\cdot 5CH_3OH\cdot 2CH_2Cl_2$ (1·sol, tppm = 4,4′,4″,4‴-tetrakis(4-pyridylethen-2-yl)tetraphenylmethane), was synthesized, which showed temperature, light and solvent-induced spin-crossover behaviours.

Electronically bistable magnetic materials possessing two or more electronic states represent an exceptionally rich field of functional materials research.[1,2] Among such materials, spin-crossover (SCO) compounds are a type of conveniently and physically addressable molecular-scale switch between the high-spin (HS) and low-spin (LS) states under external perturbations,[3,4] which may be rationalized on the basis of ligand-field theory.[5] Up to date, a large number of SCO materials have been synthesized, most of them are based on a typical local coordination structure $Fe^{II}N_6$.[6,7] However, systematic comparison of highly structure-related compounds is still very important for understanding the above-mentioned subtle effects on SCO properties.[8] Thus, rational design of these bistable molecular systems that exhibit tunable SCO behaviours is still the subject of intense worldwide research activity.

Recently, many efforts have been devoted to introduce SCO-active centers into porous coordination polymers (PCPs). Due to chemical versatility and porosity,[9–11] these polymers can serve as a suitable platform for investigating the structure–property correlations.[12] The guest molecules – whose weak intermolecular interactions and steric effect were found to affect the electronic cooperatives of SCO centers and therefore the widths of hysteresis loops – could be altered to evaluate the effect of host–host and host–guest interactions on SCO behaviours. For example, the guest molecule with smaller dielectric constant in the $[Fe(NCS)_2(bpbd)_2]\cdot$guest (bpbd = 2,3-bis(4′-pyridyl)-2,3-butanediol) gave rise to higher SCO temperature,[13] while the large guest molecule in the $[Fe(bdpt)_2]\cdot$guest (Hbdpt = 3-(5-bromo-2-pyridyl)-5-(4-pyridyl)-1,2,4-triazole) retarded framework's contraction and lowered the SCO temperature.[14]

In principle, porous coordination polymers with small cavity sizes and multiple coordination networks, such as two-dimensional (2D) and three-dimensional (3D) interpenetrated structures, can supply significant structures responsible for encapsulating different guest molecules.[15,16] To date, a few such materials have been reported based on the extension of the $\{Fe^{II}(pyridyl)_4(trans\text{-}NCS)_2\}$ chromophore using bridging exodentate pyridyl-based ligands.[9,17,18] Despite their structural similarities, these materials have a diverse range of guest-dependent structures and SCO features due in part to the structural flexibility associated with interpenetration and variance in the host–host and host–guest interactions. As our continuous studies on SCO properties of such porous materials, we select a tetradentate ligand, 4,4′,4″,4‴-tetrakis(4-pyridylethen-2-yl)tetraphenylmethane (tppm, Fig. 1a), to achieve the $\{Fe^{II}(pyridyl)_4(trans\text{-}NCS)_2\}$ chromophore and hence a 3D spin-crossover porous coordination polymer. Through introducing various guest molecules in the cavities of the framework, the effects of guest molecules on SCO behaviours have been determined.

The title complex $[Fe(NCS)_2(tppm)]\cdot 5CH_3OH\cdot 2CH_2Cl_2$ (**1**·sol) crystallized in the orthorhombic space group *Pban* at room temperature. The asymmetric unit has two half-occupancy Fe^{II} atoms lying on sites with 222-symmetry and the central carbon C14 lying on a twofold axis, each Fe^{II} atom adopts an FeN_6 octahedral coordination geometry with four pyridyl N atoms of four tppm ligands located in the basal plane and two NCS^- groups in the apical positions. The crystal structures of **1** at different temperatures were investigated. Upon decreasing the temperature, the complex underwent a phase transition from the space group of *Pban* (200 K) to that of *Pnna* (153 K, the asymmetric unit has two half-occupancy Fe^{II} atoms lying on twofold axes) with the overall topological structure remaining intact, instead relatively large variances occurred in the coordination spheres of Fe^{II} atoms. As shown in Fig. S1 and S2 and Tables S1–S3 (ESI†), the average Fe1–N and Fe2–N bond lengths are 2.085 and 2.137 Å at 200 K, which are 1.960 and 2.066 Å at 153 K, respectively. These metric values fall in the range of normal LS and HS Fe^{II}–N bond lengths of reported binuclear LS–HS and HS–HS Fe^{II}-(pyridyl) compounds.[6,14]

State Key Laboratory of Physical Chemistry of Solid Surfaces and Department of Chemistry, College of Chemistry and Chemical Engineering, Xiamen University, Xiamen 361005, People's Republic of China. E-mail: taojun@xmu.edu.cn; Fax: +86-592-2183047; Tel: +86-592-2188138

† Electronic supplementary information (ESI) available: Materials and measurements, synthesis and characterization data and supplementary figures. CCDC 950638 and 950639. For ESI and crystallographic data in CIF or other electronic format see DOI: 10.1039/c3cc45691a

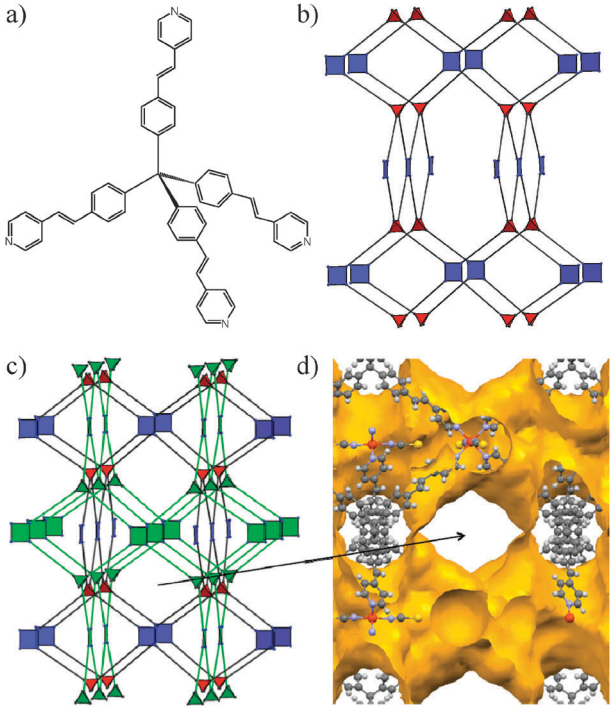

Fig. 1 Ligand tppm used in the synthesis (a), the 3D PtS-type topological structure of **1** where the ligand tppm is simplified as a tetrahedron and the {Fe^{II}(pyridyl)$_4$(*trans*-NCS)$_2$} chromophore as a square (b), the 2-fold interpenetrated structure of **1** (c), and the 1D void channel viewed along the *a* axis, where guest molecules are omitted for clarity (d).

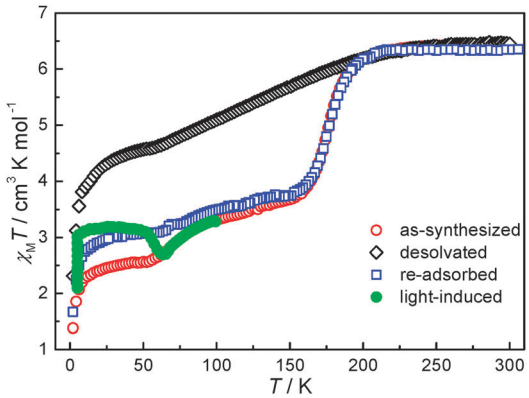

Fig. 2 Temperature dependence of $\chi_M T$ (per Fe_2 unit) for **1** (applied field: 5000 Oe, temperature range: 2–300 K). Light irradiation was carried out at 5 K by 532 nm laser light followed by thermal relaxation.

Meanwhile, the various temperature Fe–N bond lengths indicate that the Fe1 atom has undergone a complete SCO above 150 K while the Fe2 atom has not, suggesting a possible two-step SCO for **1**·5CH_3OH·2CH_2Cl_2. The topological structure of **1** can be assigned to the PtS-type (4,4)-connected 3D network with a Schäfli symbol of (4^2,8^4) when the ligand tppm is simplified as a tetrahedron and the {Fe^{II}(pyridyl)$_4$(*trans*-NCS)$_2$} chromophore as a square (Fig. 1b). The PtS-type network is self-interpenetrated in two fold, defining one-dimensional voids along the *a* axis that account for about 40% of the unit-cell volume (Fig. 1c). The identity and the number of solvent molecules residing in the voids (Fig. 1d) cannot be determined by crystallographic studies, which instead are estimated by elemental analyses (Table S4, ESI†) and thermogravimetric analyses (Fig. S4, ESI†), and the results suggest that there are five CH_3OH and two CH_2Cl_2 molecules per asymmetric unit.

Magnetic properties of **1** at different status (as-synthesized, desolvated and re-adsorbed samples, respectively) were measured in the temperature range of 2–300 K (Fig. 2). The room temperature $\chi_M T$ value of the as-synthesized sample is 6.39 cm^3 K mol^{-1}, which is consistent with the value expected for two HS Fe^{II} ions. Upon cooling, the $\chi_M T$ value remains substantially unchanged above 220 K, and then exhibits an abrupt decrease from 200 K to 153 K reaching a value of 3.65 cm^3 K mol^{-1}. After an inclined plateau, the $\chi_M T$ value continues to decrease steeply from 3.29 cm^3 K mol^{-1} at 98 K to 2.54 cm^3 K mol^{-1} at 46 K, which then gradually decreases to 2.27 cm^3 K mol^{-1} at 10 K. Thus, we can conclude that the as-synthesized complex undergoes a two-step incomplete SCO at $T_{1/2(1)}$ = 176 K and $T_{1/2(2)}$ = 72 K, respectively. The sudden drop of the $\chi_M T$ value below 10 K is mainly due to the zero-field splitting effect of residual HS Fe^{II} ions. Considering the variable temperature crystal structure, the first-step SCO can be assigned to the spin-state transition of Fe1 ion and the second-step SCO of Fe2 ion. The fully desolvated sample, however, shows rather different magnetic behavior, whose $\chi_M T$ value gradually decreases from 6.45 to 6.33 cm^3 K mol^{-1} between 300 and 224 K, then linearly decreases to 4.58 cm^3 K mol^{-1} at 54 K. The final descent of the $\chi_M T$ value can also be assigned to the zero-field splitting effect of residual HS Fe^{II} ions. The results indicate a one-step incomplete SCO for the desolvated sample with $T_{1/2}$ being 130 K, which may be attributed to the disappearance of host–guest interactions and the deformation of the framework after desolvation.[9] When the desolvated sample was immersed in CH_3OH–CH_2Cl_2 (v/v = 1 : 1) solution, the magnetic behavior of the re-adsorbed sample almost restores to the original one of the as-synthesized sample, except that a divergency occurs below 166 K. The results suggest that the framework **1** is stable enough during guest desorption–resorption and shows significant guest-dependent SCO properties. It should be noticed that no hysteresis is observed for any sample even though the SCO centers communicating with strong covalent bonds are expected to show a cooperative effect.

In order to further study the guest-dependent SCO behavior of the framework **1**, magnetic properties of **1** in various solvents were measured. As shown in Fig. 3 and Table 1, all samples show a SCO behaviour similar to that of the as-synthesized sample, but the $T_{1/2(1)}$ values span a range of about 40 K with the transition temperature following an order $T_{1/2}$(**1**·CH_3OH) < $T_{1/2}$(**1**·C_2H_5OH) < $T_{1/2}$(**1**·C_6H_{12}) < $T_{1/2}$(**1**·CH_2Cl_2) ~ $T_{1/2}$(**1**·$CHCl_3$) ~ $T_{1/2}$(**1**·CH_3CN) ~ $T_{1/2}$(**1**·CH_3COCH_3). In the present case, the effects of guest molecules on SCO of **1** can be divided into two situations: (1) protic solvent molecules such as methanol and ethanol effectively lower the transition temperatures, which are attributed to host–guest weak interactions that reduce the electron density of the host framework;[19] (2) the HS state is relatively unstable in aprotic solvents,[18,20,21] so the transition temperature of **1**·CH_2Cl_2 is higher than that of **1**·CH_3OH or **1**·C_2H_5OH. It is noteworthy that the aprotic molecule cyclohexane can also stabilize the HS state, which may be due to its large molecular volume that prevents the framework from contraction.[22]

Furthermore, we speculate that the reason for the $T_{1/2(1)}$ value of **1**·CH_3OH being lower than that of **1**·C_2H_5OH is the

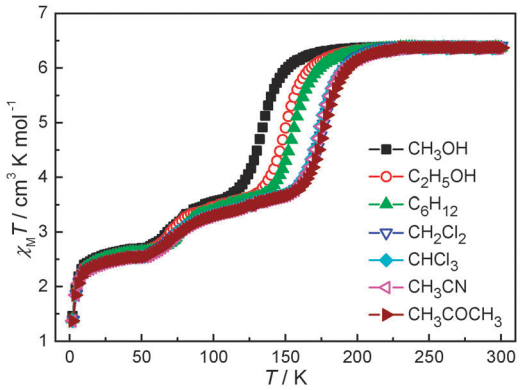

Fig. 3 $\chi_M T$ *versus* T plots for **1** as a function of solvents (applied field: 5000 Oe, temperature range: 2–300 K). C_6H_{12} is cyclohexane.

Table 1 SCO temperatures and guest-molecule volumes[22,23] for **1**·guest, where the guest is CH_3OH, C_2H_5OH, C_6H_{12}, CH_2Cl_2, $CHCl_3$, CH_3CN and CH_3COCH_3, respectively

	$T_{1/2(1)}$/K	Guest volume/Å^3
1·CH_3OH	134	40.9
1·C_2H_5OH	150	60.0
1·C_6H_{12}	156	101.1
1·CH_2Cl_2	176	56.3
1·$CHCl_3$	177	69.9
1·CH_3CN	175	52.3
1·CH_3COCH_3	177	64.4

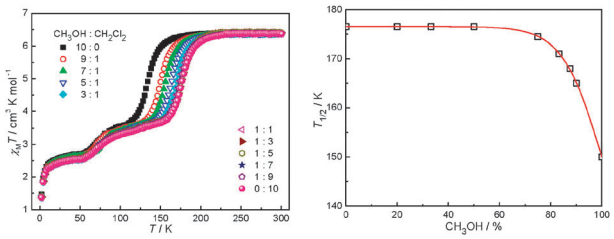

Fig. 4 $\chi_M T$ *versus* T plots for **1** as a function of CH_3OH/CH_2Cl_2 ratio (left) and $T_{1/2}$ *versus* volume percentage of CH_3OH in CH_3OH/CH_2Cl_2 solution (right). The solid red line represents the best nonlinear regression fit of the data.

smaller size of CH_3OH, which can be more included in the framework (confirmed by elemental analysis) and therefore bring more weak interactions. To quantitatively illustrate the correlation between $T_{1/2(1)}$ and the amount of methanol, magnetic measurements on **1** with various CH_3OH/CH_2Cl_2 ratios were conducted. The $T_{1/2(1)}$ value clearly shifts to high temperature upon decreasing the CH_3OH–CH_2Cl_2 ratio from 10 : 0 to 3 : 1 (Fig. 4, left), while the $T_{1/2(1)}$ value remains approximately constant when CH_3OH is less than half of the solution. When the amount of CH_3OH exceeds 70%, the $T_{1/2(1)}$ value dramatically decreases, indicating that the protic solvent molecules in **1** cannot effectively modify the SCO properties until they are in a high proportion.

A preliminary light-induced excited spin-state trapping (LIESST) experiment was also carried out (Fig. 2). Upon irradiation with a green light (532 nm, 150 mW) for 2 h at 5 K, the $\chi_M T$ value of the as-synthesized sample increases from 2.10 cm^3 K mol^{-1} to 3.01 cm^3 K mol^{-1}, clearly suggesting that the metastable HS state can be partially trapped (*ca.* 18.3% photoexcitation). After the light is switched off, the $\chi_M T$ value smoothly increases upon warming to reach a value of 3.19 cm^3 K mol^{-1} at 25 K owing to the zero-field splitting effect of HS Fe^{II} ions. The metastable state is readily accessible up to 47 K, after which the initial magnetic susceptibility is gradually restored at 61 K. This behaviour suggests that only the Fe^{II} ion involving incomplete SCO behaviour (*i.e.* Fe2) in this system can be effectively trapped at the HS metastable state.

In conclusion, we have synthesized a 3D porous coordination polymer and investigated its temperature, light and solvent-induced SCO properties. The results indicate that the incorporation of SCO-active $Fe^{II}N_6$ units into sophisticated framework structures by large bridging ligands may lead to technologically interesting materials cooperative in their physical properties.

Notes and references

1 J. S. Miller, *Inorg. Chem.*, 2000, **39**, 4392–4408.
2 J. S. Miller and M. Drillon, *Magnetism II: Molecules to Materials*, Wiley-VCH, Weinheim, Germany, 2002.
3 O. Kahn, *Molecular Magnetism*, VCH, New York, 1993.
4 P. Gütlich and H. Goodwin, in *Spin Crossover in Transition Metal Compounds I*, ed. P. Gütlich and H. A. Goodwin, Springer Berlin Heidelberg, 2004, vol. 233, pp. 1–47.
5 A. Hauser, in *Spin Crossover in Transition Metal Compounds I*, ed. P. Gütlich and H. A. Goodwin, Springer Berlin Heidelberg, 2004, vol. 233, pp. 49–58.
6 J. Olguín and S. Brooker, *Coord. Chem. Rev.*, 2011, **255**, 203–240.
7 M. C. Muñoz and J. A. Real, *Coord. Chem. Rev.*, 2011, **255**, 2068–2093.
8 X. Bao, J.-L. Liu, J.-D. Leng, Z. Lin, M.-L. Tong, M. Nihei and H. Oshio, *Chem.–Eur. J.*, 2010, **16**, 7973–7978.
9 S. M. Neville, G. J. Halder, K. W. Chapman, M. B. Duriska, P. D. Southon, J. D. Cashion, J.-F. Létard, B. Moubaraki, K. S. Murray and C. J. Kepert, *J. Am. Chem. Soc.*, 2008, **130**, 2869–2876.
10 S. Kitagawa and R. Matsuda, *Coord. Chem. Rev.*, 2007, **251**, 2490–2509.
11 S. Horike, R. Matsuda, D. Tanaka, S. Matsubara, M. Mizuno, K. Endo and S. Kitagawa, *Angew. Chem., Int. Ed.*, 2006, **45**, 7226–7230.
12 Y. Garcia, F. Robert, A. D. Naik, G. Zhou, B. Tinant, K. Robeyns, S. Michotte and L. Piraux, *J. Am. Chem. Soc.*, 2011, **133**, 15850–15853.
13 S. M. Neville, G. J. Halder, K. W. Chapman, M. B. Duriska, B. Moubaraki, K. S. Murray and C. J. Kepert, *J. Am. Chem. Soc.*, 2009, **131**, 12106–12108.
14 J.-B. Lin, W. Xue, B.-Y. Wang, J. Tao, W.-X. Zhang, J.-P. Zhang and X.-M. Chen, *Inorg. Chem.*, 2012, **51**, 9423–9430.
15 J.-P. Zhang, Y.-Y. Lin, W.-X. Zhang and X.-M. Chen, *J. Am. Chem. Soc.*, 2005, **127**, 14162–14163.
16 A. Kondo, H. Kajiro, H. Noguchi, L. Carlucci, D. M. Proserpio, G. Ciani, K. Kato, M. Takata, H. Seki, M. Sakamoto, Y. Hattori, F. Okino, K. Maeda, T. Ohba, K. Kaneko and H. Kanoh, *J. Am. Chem. Soc.*, 2011, **133**, 10512–10522.
17 S. M. Neville, B. Moubaraki, K. S. Murray and C. J. Kepert, *Angew. Chem., Int. Ed.*, 2007, **46**, 2059–2062.
18 G. J. Halder, C. J. Kepert, B. Moubaraki, K. S. Murray and J. D. Cashion, *Science*, 2002, **298**, 1762–1765.
19 C. T. Brewer, G. Brewer, R. J. Butcher, E. E. Carpenter, A. M. Schmiedekamp, C. Schmiedekamp, A. Straka, C. Viragh, Y. Yuzefpolskiy and P. Zavalij, *Dalton Trans.*, 2011, **40**, 181–194.
20 B. A. Leita, B. Moubaraki, K. S. Murray and J. P. Smith, *Polyhedron*, 2005, **24**, 2165–2172.
21 P. Gütlich, Y. Garcia and H. A. Goodwin, *Chem. Soc. Rev.*, 2000, **29**, 419–427.
22 P. D. Southon, L. Liu, E. A. Fellows, D. J. Price, G. J. Halder, K. W. Chapman, B. Moubaraki, K. S. Murray, J.-F. Létard and C. J. Kepert, *J. Am. Chem. Soc.*, 2009, **131**, 10998–11009.
23 C. E. Webster, R. S. Drago and M. C. Zerner, *J. Am. Chem. Soc.*, 1998, **120**, 5509–5516.